Heterodyne common-path grating interferometer with Littrow configuration

Chyan-Chyi Wu,[1,*] Cheng-Chih Hsu,[2] Ju-Yi Lee,[3] and Yan-Zou Chen[1,4]

[1] *Department of Mechanical and Electromechanical Engineering, Tamkang University, Taiwan*
[2] *Department of Photonics, Yuan-Ze University, Taiwan*
[3] *Institute of Optomechatronics, National Central University, Taiwan*
[4] *Institute of Mechanical Engineering, National Taiwan University, Taiwan*
** chyanchyi@gmail.com*

Abstract: This paper presents a heterodyne common-path grating interferometer with Littrow configuration (HCGIL). The HCGIL can effectively overcome environmental disturbance effect and the DC offset and the amplitude variation of the measurement signals. Experimental results match well with the HP5529A results for long-range measurements. Results also show that the estimated measurement resolution is 0.15 ± 0.027 nm. The stability of the HCGIL is −0.41 ± 0.23 nm. Therefore, the HCGIL has potential for subnanometer resolution and long-range applications.

OCIS codes: (120.0120) Instrumentation, measurement, and metrology; (120.3180) Interferometry.

References and links

1. http://www.itrs.net.
2. C.-C. Wu, W.-J. Wu, Z.-S. Pan, and C.-K. Lee, "Laser linear encoder with both high fabrication and head-to-scale tolerances," Appl. Opt. **46**(16), 3169–3176 (2007).
3. C. F. Kao, S. H. Lu, H. M. Shen, and K. C. Fan, "Diffractive laser encoder with a grating in littrow configuration," Jpn. J. Appl. Phys. **47**(3), 1833–1837 (2008).
4. F. Cheng and K.-C. Fan, "Linear diffraction grating interferometer with high alignment tolerance and high accuracy," Appl. Opt. **50**(22), 4550–4556 (2011).
5. C.-C. Hsu, Y.-Y. Sung, Z.-R. Lin, and M.-C. Kao, "Prototype of a compact displacement sensor with a holographic diffraction grating," Opt. Laser Technol. **48**, 200–205 (2013).
6. S. J. Friedman, B. Barwick, and H. Batelaan, "Focused-laser interferometric position sensor," Rev. Sci. Instrum. **76**(12), 123106 (2005).
7. H. L. Hsieh, J. Y. Lee, W. T. Wu, J. C. Chen, R. Deturche, and G. Lerondel, "Quasi-common-optical-path heterodyne grating interferometer for displacement measurement," Meas. Sci. Technol. **21**(11), 115304 (2010).
8. J.-Y. Lee and M.-P. Lu, "Optical heterodyne grating shearing interferometry for long-range positioning applications," Opt. Commun. **284**(3), 857–862 (2011).
9. C. C. Wu, J. S. Yang, C. Y. Cheng, and Y. Z. Chen, "Common-path laser encoder," Sens. Actuat. A **189**, 86–92 (2013).
10. P. L. M. Heydemann, "Determination and correction of quadrature fringe measurement errors in interferometers," Appl. Opt. **20**(19), 3382–3384 (1981).
11. C.-C. Wu, C.-H. Liao, Y.-Z. Chen, and J.-S. Yang, "Common-path Laser Encoder with Littrow Configuration," Sens. Actuat. A **193**, 69–78 (2013).
12. C.-K. Lee, C.-C. Wu, S.-J. Chen, L.-B. Yu, Y.-C. Chang, Y.-F. Wang, J.-Y. Chen, and J. W.-J. Wu, "Design and construction of linear laser encoders that possess high tolerance of mechanical runout," Appl. Opt. **43**(31), 5754–5762 (2004).
13. D.-C. Su, M.-H. Chiu, and C.-D. Chen, "Simple two-frequency laser," Precis. Eng. **18**(2-3), 161–163 (1996).
14. C.-M. Wu and R. D. Deslattes, "Analytical modeling of the periodic nonlinearity in heterodyne interferometry," Appl. Opt. **37**(28), 6696–6700 (1998).
15. A. J. Fleming, "A review of nanometer resolution position sensors: operation and performance," Sens. Actuat. A **190**, 106–126 (2013).

1. Introduction

Continuing rapid progress in many advanced manufacture technologies such as the semiconductor, liquid crystal display (LCD), micro- and nano-technology, has built a

#186589 - $15.00 USD Received 7 Mar 2013; revised 15 May 2013; accepted 17 May 2013; published 24 May 2013

challenge for measurement technology used in these fields. Especially, 23-nm node over a 450-mm wafer is expected soon in 2016 [1]. The displacement measurement of nano- or subnanometer resolution over such a large area is required to meet this node technology. As the laser encoder or grating interferometer transfers the measurement scale from the laser wavelength into the grating pitch, it can offer better immunity to environmental disturbances than the laser interferometer [2]. Many studies on the grating interferometer have been reported in past a decade [2–5]. Note that these grating interferometers are in non-common-path configurations. Inevitably, the measurement resolution and stability of these grating interferometers are spoiled by environmental disturbances. Practically, to attain a displacement measurement of nanometer or smaller resolution over a long range, the grating interferometer must be operated in a strictly controlled environment, for example in vacuum with very small variations in temperature, pressure and humidity, but at the price of high cost. However, there are few publications on overcoming the environmental disturbance effect on the grating interferometer. Friedman et al. proposed a focused-laser grating interferometer which especially has a common-path configuration [6]. It used a grating to produce a shearing interference and the grating displacement can be measured from the interference fringe variation. This grating interferometer is essentially immune to environmental disturbances. However, it used a single photodetector to measure the fringe movement which stems from the grating movement, so it cannot distinguish the direction of displacements. Based on the shearing interference principle, Hsieh et al. proposed quasi-common-path grating interferometer (QCOP) with a heterodyne laser source [7]. The QCOP combined the shearing interference technique and the polarization interferometry. It has good immunity to environmental disturbances. The stability of the QCOP is about 14 nm/h. The resolution of the QCOP is about 1.2 nm. Lee and Lu demonstrated a heterodyne grating interferometer with a quasi-common-path configuration [8]. Their grating interferometer has a measurement resolution of 2.3 nm over a 20-mm range. In our previous work, we presented a common-path laser encoder (CPLE) [9]. The CPLE has a measurement resolution of 0.1 ± 0.046 nm. In a general laboratory condition, its stability is about 5.5 nm/h, which is twenty times better than that of the HP5529A. However, as the CPLE is a type of the homodyne grating interferometer, its measurement resolution and then accuracy are subject to the DC offset and the amplitude variation of the output signal waveforms [10]. In order to further improve the measurement performance of the grating interferometer, the DC offset and the amplitude variation must be slashed. In our previous work, we demonstrated a common-path laser encoder with Littrow configuration (CPLi) [11]. We showed that a Littrow configuration combined with an 1-x telescope can effectively raise the head-to-scale tolerance which is essential to the laser encoder for wide applications. The CPLi has runout tolerance of 1.5 to 3 times greater than that of our previous work [12]. The CPLi provides a measurement resolution of 0.12 ± 0.021 nm. Its system stability is as low as −0.25 ± 0.098 nm/h.

This paper presents a heterodyne common-path grating interferometer with Littrow configuration (HCGIL). The HCGIL can effectively overcome environmental disturbance effect and the DC offset and the amplitude variation of the measurement signals. As the HCGIL adopts a Littrow configuration and an 1-x telescope configuration, it can provide a high head-to-scale tolerance. The operation principle of the HCGIL are detailed. Experimental results show that the HCGIL has a resolution of 0.15 ± 0.027 nm and a stability of −0.41 ± 0.23 nm/h. These results demonstrate that the HCGIL can measure short- and long- range displacements with subnanometric resolution. The HCGIL is a promising method for nanometer or subnanometer positioning applications.

#186589 - $15.00 USD Received 7 Mar 2013; revised 15 May 2013; accepted 17 May 2013; published 24 May 2013

2. Principle

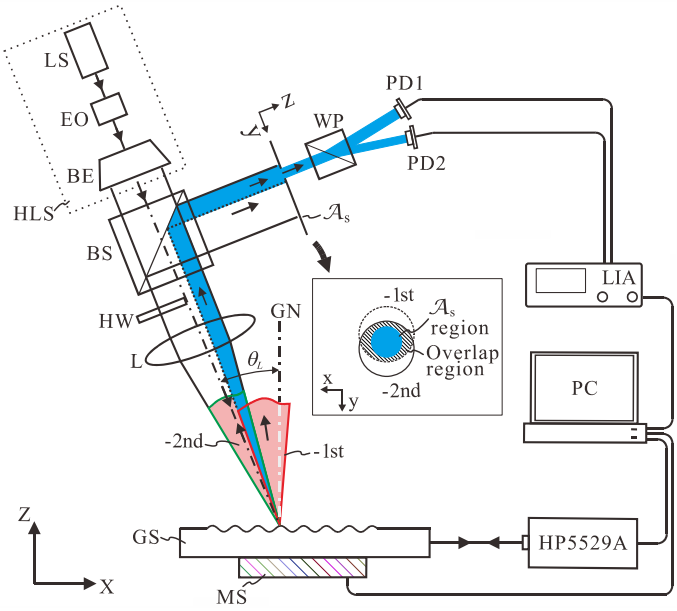

Fig. 1. Schematics of the HCGIL configuration and experimental setup. LS: laser source; EO: electro-optic modulator; BE: beam expander; HLS: heterodyne laser source; BS: beam splitter; HW: half-wave plate; L: lens; GS: grating scale; MS: moving stage; A_s: aperture stop; WP: Wollaston polarizer; PD1 and PD2: photodetectors; LIA: lock-in amplifier; PC: personal computer; GN: grating normal.

The schematic diagram of the HCGIL configuration is shown in Fig. 1. A heterodyne laser source (HLS) consists of a laser source (LS), and an electro-optic modulator (EOM) driven by a function generator (FG) [13], and a beam expander (BE). A half-wave plate (HW) transfers the polarization of a part of the HLS to make the polarization orthogonal to the left part of the HLS. The HLS then passes through a focusing lens (L) and becomes a focused beam with the focus point on the grating scale (GS). This focused beam incidents on the GS and is diffracted. Accordingly, we have a −1st and a −2nd order diffracted beams, which are divergent. These two diffracted beams pass through the L again and become two collimated beams. These two collimated beams overlap partially. Then these two overlapped 0th and 2nd order diffracted beams pass through the aperture stop ($\mathcal{A}_s$) and traverse to a Wollaston polarizer (WP) in common-path. Finally, the p- and s-polarization components of these two common-path beams are interfered respectively. The interference signal of the p-polarization components is received by the photodetectors PD1, and the interference signal of the s-polarization components is received by the photodetectors PD2. According to the Jones calculus, the electric fields of p- and s-polarizations of 0th and −2nd order diffracted beams after collimated by the L can be expressed as follows:

$$E_{\mathrm{p},-1} = \alpha_{\mathrm{p},-1} \cdot e^{j(\omega_0+\omega/2)t}, \tag{1}$$

$$E_{\mathrm{s},-1} = \alpha_{\mathrm{s},-1} \cdot e^{j(\omega_0-\omega/2)t}, \tag{2}$$

$$E_{\mathrm{p},-2} = \alpha_{\mathrm{p},-2} \cdot e^{j\left[(\omega_0-\omega/2)t+\phi_{\mathrm{p}}\right]}, \tag{3}$$

$$E_{\mathrm{s},-2} = \alpha_{\mathrm{s},-2} \cdot e^{j\left[(\omega_0+\omega/2)t+\phi_{\mathrm{s}}\right]}, \tag{4}$$

#186589 - $15.00 USD Received 7 Mar 2013; revised 15 May 2013; accepted 17 May 2013; published 24 May 2013

where $\alpha_{p,-1}$, $\alpha_{s,-1}$, $\alpha_{p,-2}$, and $\alpha_{s,-2}$ are the diffraction coefficients for the p- and s- components of −1st and −2nd order diffraction beams, ω_0 is the frequency of the LS (see Fig. 1), ω is the modulation frequency of the EOM (see Fig. 1), ϕ_p and ϕ_s are the phase shifts of p- and s-components respectively when the light beam is diffracted by the moving GS (see Fig. 1), and $j=\sqrt{-1}$. After passing through the WP, $E_{p,-1}$ and $E_{p,-2}$ are directed to the PD1; $E_{s,-1}$ and $E_{s,-2}$ are directed to the PD2. Therefore, the intensities I_1 and I_2 which are measured by the PD1 and PD2 respectively can be expressed as follows:

$$I_1 \propto \alpha_{p,-1}^2 + \alpha_{p,-2}^2 + 2\alpha_{p,-1}\alpha_{p,-2}\cos\left(\omega t - \phi_p\right), \tag{5}$$

$$I_2 \propto \alpha_{s,-1}^2 + \alpha_{s,-2}^2 + 2\alpha_{s,-1}\alpha_{s,-2}\cos\left(\omega t + \phi_s\right). \tag{6}$$

Generally, $\alpha_{p,-1}=\alpha_{s,-1}$, $\alpha_{p,-2}=\alpha_{s,-2}$ and $\phi_p=\phi_s=\phi$. These two sinusoidal signals are sent into a lock-in amplifier (LIA) or phase meter for phase difference measurement and the total phase shift $\Delta\Phi$ between I_1 and I_2 can be obtained and expressed as

$$\Delta\Phi = 2\phi = \frac{4\pi}{\rho}\Delta X. \tag{7}$$

Based on the relationship in Eq. (7), the measured displacement, ΔX, can be written as

$$\Delta X = \frac{\Delta\Phi}{4\pi}\rho, \tag{8}$$

where ρ is the grating pitch. That is, the grating displacement ΔX can be determined by measuring the phase difference $\Delta\Phi$ between the two sinusoidal signals and the known grating pitch ρ. The angle of incidence of the laser source, θ_L (see Fig. 1), can be determined using the grating equation as follows:

$$\theta_L = \sin^{-1}\frac{\lambda}{\rho}. \tag{9}$$

Here θ_L is about 23.3° with λ = 632.8 nm, ρ = 1.6 μm.

3. Experiments and results

A stabilized He-Ne laser with a wavelength of 632.991 nm (in vacuum) was used as the laser source of the HCGIL. An EOM (model: 4001, New Focus Inc.) was driven by a function generator with a 20-kHz sawtooth input signal. The focal length of the L is 12 mm, the area illuminated over the grating scale has a diameter of about half a millimeter, and the diameter of the $\mathcal{A}_s$ is about 1.8 mm. A sinusoidal surface-relief grating scale with a pitch of 1.6 μm and a measuring length of 310 mm (model: BL57-031RE, Sony Precision Technology Inc.) was mounted on a composite nanopositioning stage. The composite nanopositioning stage composed of a 100 mm-range coarse motorized stage (model: ALS-510-H1P, Chuo Precision Industrial Co. Ltd.) with a laser encoder (model: Mercury II SP4800, MicroE Inc.) of 1.2-nm resolution for the displacement feedback and a 100 μm-range fine piezoelectric stage (model: P-611.3S, Physik Instrumente Inc.). The composite nanopositioning stage was pre-calibrated by a HP5529A laser interferometer. The coarse motorized stage provided a 10-nm minimum incremental motion. The straightness and flatness of the linear guide rail was guaranteed by 1 μm per 100 mm. The fine stage has a positioning resolution of 0.1 nm. An all-digital FPGA (field programmable gate array) based lock-in amplifier (LIA) was developed to real-time

#186589 - $15.00 USD Received 7 Mar 2013; revised 15 May 2013; accepted 17 May 2013; published 24 May 2013

implement the phase demodulation to 20 MHz. The LIA has two analog output ports. The decoded phase signal were sent into a high-speed PCI-DIO card installed on a personal computer (PC) to implement the phase unwrapping and displacement calculations. The setup of the optical layout was placed on the isolated optical table (model: RS 1000, Newport Inc.) to prevent low frequency noise from the foundation motion. The laboratory conditions were monitored using the HP5529A. The average atmosphere temperature was 26.2 °C with a standard deviation of 0.54 °C. The average atmosphere pressure was 761.3 mm-Hg with a standard deviation of 0.52 mm-Hg.

3.1 Long-range measurements

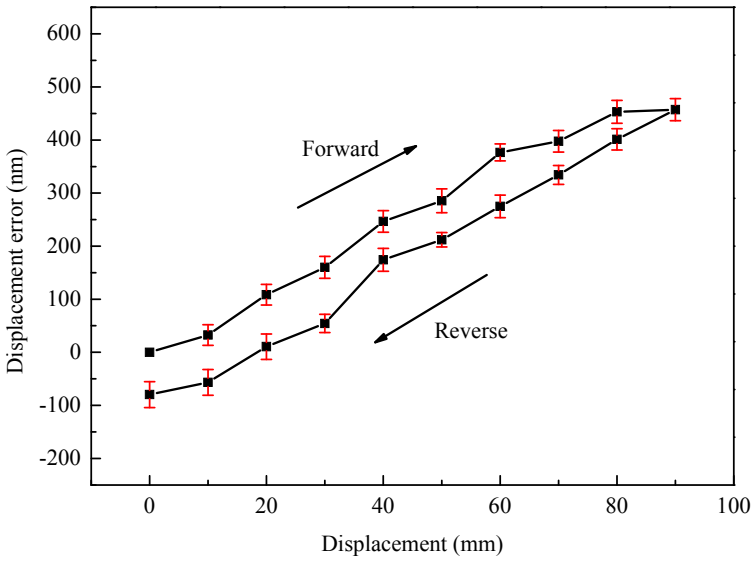

Fig. 2. Measurement result of the 90-mm long-range for the HCGIL compared with the HP5529A.

To verify the measurement performance of the HCGIL for long-range displacements, we turned off the fine stage and used the coarse stage only in such long-range experiments. The reference displacement of the coarse stage relies on the reading of the HP5529A.

The first experiment is a forward-and-backward measurement of a 90-mm range. We repeated this experiment five times. We compared the readings of the HP5529A and the HCGIL respectively at 10, 20, 30, 40, 50, 60, 70, 80, 90 mm displacements. The home position was determined based on the built-in laser encoder of the coarse stage. We calculated the average and the standard deviation for the measurement results. The result is shown in Fig. 2. Two measurement results are in good agreement. Thus, the HCGIL is able to measure a long-range displacement. In Fig. 2, the maximum average displacement error between the HP5529A and the HCGIL was 458.6 nm, and happened at 90-mm displacement. According to the work by Wu et al. [14], the nonlinear cyclic error is in the scale of ten nanometers. We might deduce that the error in the result of Fig. 2 should come mainly from the cosine error and the drift effect of the HP5529A and the HCGIL. Drift is related to stability, and we will study the stability of the HCGIL in Section 3.4. The repeatability behavior depends on the resolutions of the HP5529A and the HCGIL, and will be discussed in Section 4.3.

#186589 - $15.00 USD Received 7 Mar 2013; revised 15 May 2013; accepted 17 May 2013; published 24 May 2013

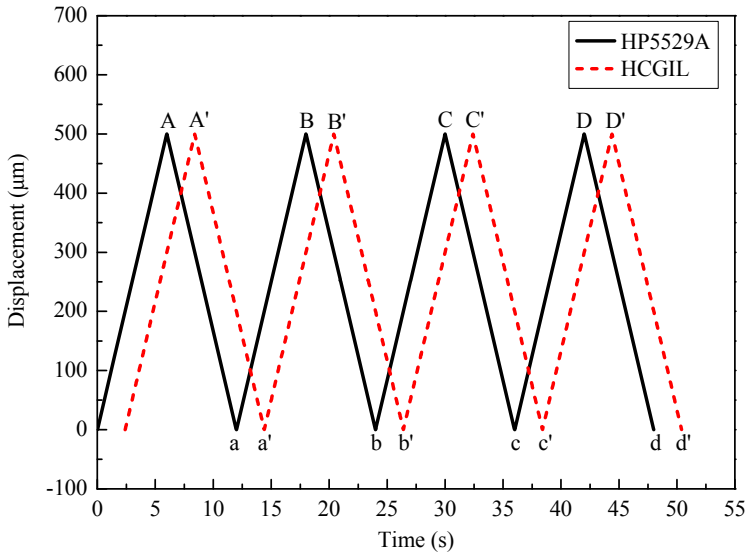

Fig. 3. Measurement result of cyclic 500-μm movement using the HP5529A and the HCGIL.

Table 1. Peak values of the HP5529A and the HCGIL for the experiment of a 500-μm cyclic movement

Position	Displacement (μm)	
A / A′	500.020	500.0070
B / B′	500.057	500.0205
C / C′	500.096	500.0344
D / D′	500.133	500.0412
a / a′	0.036	0.0136
b / b′	0.074	0.0273
c / c′	0.114	0.0342
d / d′	0.153	0.0308

In the experiment of a 500-μm range, we drove the coarse stage to move forward and backward cyclically. Figure 3 is the measurement result of cyclic 500-μm movement using the HP5529A and the HCGIL. Two curves have been shifted deliberately 2.4 s to distinguish the measurement results obtained by the HCGIL and the HP5529A. The peak values of two curves are listed in Table 1. In Fig. 3, the HP5529A and the HCGIL gives almost the same displacement waveforms. The peak-to-peak values of the HP5529A and the HCGIL are 500.002 μm ± 24 nm and 500.0008 μm ± 6.8 nm respectively.

#186589 - $15.00 USD Received 7 Mar 2013; revised 15 May 2013; accepted 17 May 2013; published 24 May 2013

3.2 Short-range measurements

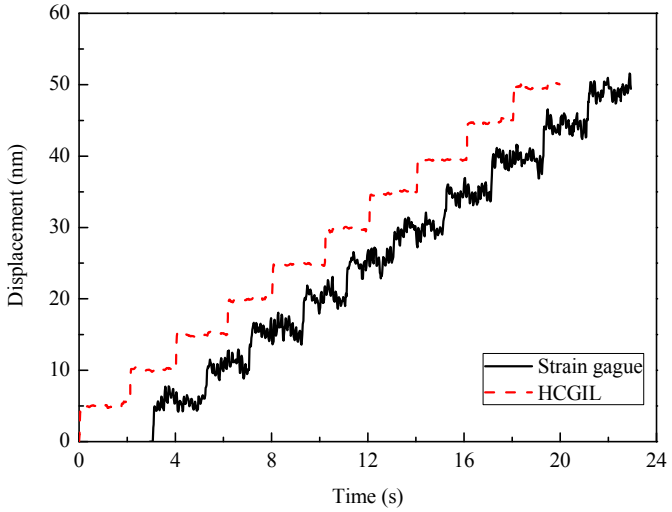

Fig. 4. Measurement result of 5-nm step movement with a total displacement of 50 nm.

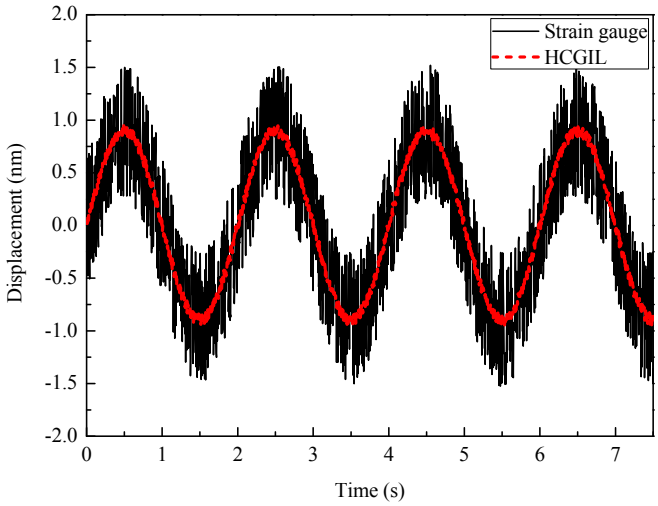

Fig. 5. Measurement results of 1.6-nm range sinusoidal movements by the HCGIL and the strain gauge.

To verify the HCGIL measurement capability on the nanometer scale, we drove the fine stage in step movement, with 1 nm for each step movement. The HCGIL and the strain gauge of the fine stage recorded the displacement variations of the GS at the same time. Figure 4 shows the displacements with time of the HCGIL and the strain gauge of the fine stage for 5-nm step movement. The dashed line in the figure was deliberately biased about 3 s on the time axis in order to distinguish the results of the HCGIL and the strain gauge. The total displacement range for this 5-nm step movement is 10 nm. Although the measurement resolution of the strain gauge is about 1 nm, it suffers from a lot of noises. Therefore, the strain gauge sensor cannot read the detailed step motion.

In order to further investigate the HCGIL measurement capability on the subnanometer scale, we drove the fine stage with a sinusoidal voltage input to the stage driver to move the GS in a harmonic motion with an amplitude of 0.8 nm. Again, we compared the result of the

#186589 - $15.00 USD Received 7 Mar 2013; revised 15 May 2013; accepted 17 May 2013; published 24 May 2013

HCGIL with that of the strain gauge. Practically, the resolution of the strain gauge is between 1 nm and 2 nm. A device with such a resolution cannot measure a displacement range near the resolution value, for example 1 nm. Figure 5 presents the measurement results of 1.6-nm range sinusoidal movements by the HCGIL and the strain gauge. We can observe that the strain gauge cannot provide detailed displacement information because the noise level of the strain gauge is too large for such a range measurement. These results confirm that the HCGIL is able to measure subnanometer displacement.

3.3 Transient motion measurement

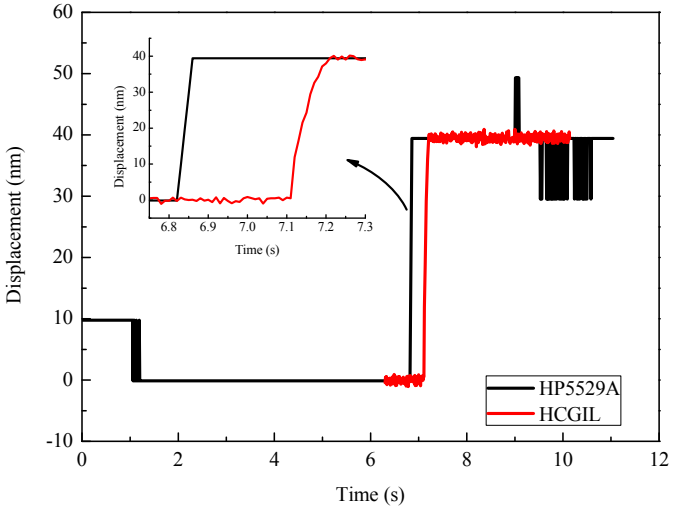

Fig. 6. The measurement result of a transient motion of a 45-nm step.

The transient performance of a nanopositioning stage is an important specification. However, it is difficult to learn the physical specification using existing measurement equipment. We drove the fine stage to move the GS a step motion of 45 nm and turned off the coarse stage electrically. In this experiment, the HP5529A started recording the displacement before the HCGIL started measuring the displacement of the GS. After the HCGIL stopped measurement, the HP5529A still continued monitoring the displacement of the GS. The measurement result of a transient motion of a 45-nm step is shown in Fig. 6. The plot of the HCGIL is deliberately shifted about 0.3 s to conveniently distinguish two curves. From Fig. 6, we can find that there are a lot of "jumps" and many seconds for the GS in stationary for the HP5529A data. Besides, from the inset of Fig. 6, the HP5529A data demonstrate that the velocity of the GS is constant in the step motion. All these phenomena from the HP5529A data are physically unreasonable. In contrast, the HCGIL can give much more detailed transient information of the GS than that the HP5529A gives. Note that the positioning resolution of the fine stage is in between 1 nm to 2 nm.

#186589 - $15.00 USD Received 7 Mar 2013; revised 15 May 2013; accepted 17 May 2013; published 24 May 2013

3.4 Stability

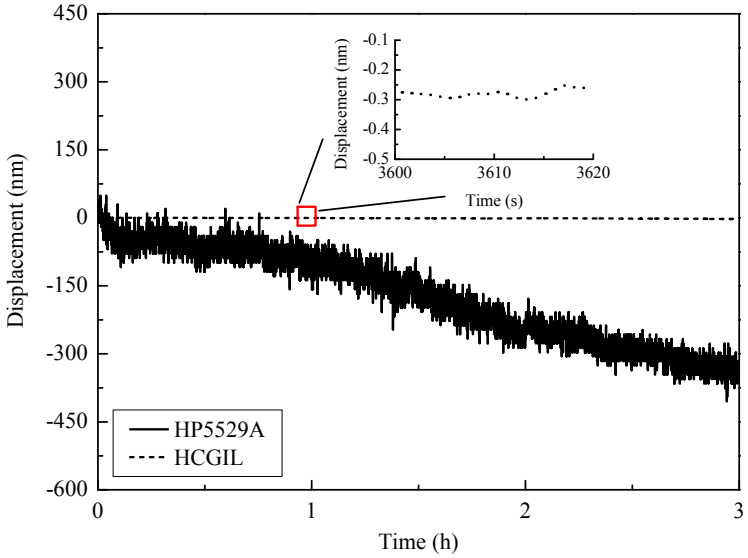

Fig. 7. The system stability measurement result for the HCGIL and the HP5529A for 3 h. The inset is the HCGIL data from 3600 s to 3620 s.

To verify the stability of the HCGIL, which reflects its immunity to environmental disturbances, we immobilized the composite nanopositioning stage carrying the GS for three hours. The two drivers of the fine and coarse stages were turned off electrically. We used the HCGIL and the HP5529A to monitor the displacement variation of the GS. Theoretically, there should be no displacement for the GS for this experiment. Figure 7 shows the system stability measurement results for the HCGIL and the HP5529A within three hours. Results show that the HCGIL data has a stability of -0.41 ± 0.23 nm/h, which is substantially smaller over two orders of magnitude than that indicated by the HP5529A data. The HCGIL data physically reflect the state of the GS. The inset of Fig. 7 shows the HCGIL data from 3600 s to 3620 s. Figure 7 explains why a laser interferometer is an improper choice for nanoscale displacement measurements in common engineering environments. In addition, the system drift of the HCGIL is two orders of magnitude smaller than that of the HP5529A in such environmental conditions within three hours. Note that HP5529A has been used as the length standard for all measurements. HP5529A can offer excellent measurement performance only if thermal effect is small or environmental conditions are strictly controlled.

4. Discussion

4.1 Sensitivity

From Eq. (8), we have the measurement sensitivity of the HCGIL as follows:

$$\frac{\Delta\Phi}{\Delta X} = \frac{4\pi}{\rho}. \tag{10}$$

In our experiments, the grating pitch used is 1.6 μm. From Eq. (10), the measurement sensitivity ($\Delta\Phi/\Delta X$) of the HCGIL is 0.45 °/nm. Physically, there are many high and low frequency phase noises for the HCGIL. The high-frequency phase noises may come from the laser source, EOM, photodetectors or other electronic components. The low-frequency phase noises may come from the foundation vibration, thermal drift, optics nonlinearity or air disturbances. Note that the grating pitch variation may also contribute to the displacement

#186589 - $15.00 USD Received 7 Mar 2013; revised 15 May 2013; accepted 17 May 2013; published 24 May 2013

measurement error. All above-mentioned factors influence the sensitivity of the HCGIL. From the design view, we can choose a smaller grating pitch in order to have a higher sensitivity as well as a smaller measurement error. This fact can be easily understood from the total differentiation of Eq. (8).

4.2 Resolution

The interpolation electronics is a way to raise the resolution, if the output signals have good quality. Under environmental disturbances, a higher interpolation factor will not give a more useful result. Therefore, the common interpolation factor is 200 or 400 only. Note that there is no international standard for the measurement or reporting of resolution in a positioning system [15].

We take a constant time interval for the resolution estimation. The constant time interval depends on the time to complete each experiment. As each experimental measurement is done within 60 s for this manuscript, we may safely or conservatively take 180 s to proceed the resolution estimation. The time axis of Fig. 7 can be divided equally into 60 segments; a left segment with time interval smaller than 180 s is not included for the resolution estimate. For each 180-s time interval, we can have a maximum and a minimum displacement values, under the stage is kept still. And all displacement values between the maximum and the minimum for each time segment are the displacements which the laser encoder cannot correctly measure. For example, the maximum and the minimum are 1 nm and −2.5 nm respectively in a 180-s time segment, we can have a resolution of 3.5 nm for this time segment. Thus, we can have 60 resolution data for these 60 time segments. The average and the standard deviation of these 60 resolution values are adopted to indicate the resolution estimate. This is the resolution limit or the resolution of the laser encoder. Note that the standard deviation of a set of data is substantially smaller than the difference between the extreme values. Practically, it may be more reasonable and reliable to take certain times of standard deviation as the resolution estimate [15]. We adopted a more strict view for the resolution estimate of the HCGIL rather than the view of standard deviation. In this way, we have the resolutions of the HCGIL and the HP5529A, 0.15 nm ± 27 pm and 102 nm ± 18.7 nm respectively. Note that the drift effect must be considered in the resolution estimate in order to really reflect the system resolution ability. Both drift and noises are recorded in Fig. 7. The only difference relies on the fact that the drift effect and noises for the HCGIL are much smaller than the ones for the HP5529A in the same laboratory environment.

4.3 Repeatability

From Fig. 7, the drift effect of the HP5529A is within tens of nanometers for all displacement measurements in this paper. For the long-range displacement measurement of Fig. 2, such drift effect is at least three orders of magnitude smaller than the measured displacements, so we can reasonably adopt the HP5529A to serve as the reference in our laboratory conditions.

The repeatability result of the HCGIL for long-range measurements was shown in Fig. 2. The maximum average error is 458.6 nm and occurs at the displacement of 90 mm, and the corresponding repeatability is ± 20.8 nm. In Fig. 2, the worst repeatability is ± 24.4 nm and the best repeatability ± 11.3 nm. Note that the repeatability of measured data depends on the in-line resolutions of the HP5529A and the HCGIL. As the time interval between two adjacent measured positions is short, the repeatability measurement results are dominated by the in-line resolution of the HP5529A. From Fig. 7, the short-term resolution of the HP5529A within 8 sec can be estimated to be 20 nm ± 0.4 nm. From Fig. 7, we can also see that the later measured positions will have larger errors although they might have good repeatability.

5. Conclusion

We present the HCGIL with a common-path configuration so that the HCGIL has superior immunity to environmental disturbances. The HCGIL adopts a Littrow configuration and an

#186589 - $15.00 USD Received 7 Mar 2013; revised 15 May 2013; accepted 17 May 2013; published 24 May 2013

1-x telescope configuration, it can provide a high head-to-scale tolerance. As the HCGIL adopts heterodyne detection, it can effectively overcome the common problem of DC offset and amplitude variation for the homodyne grating interferometer. The experimental results of long-range displacement measurements match well with the commercial HP5529A laser interferometer. The HCGIL has subnanometer displacement measurement resolution. The HCGIL can provide more detailed behavior of nanometer scale short-range displacement measurements than the built-in strain gauge. The estimated measurement resolution and the stability of the HCGIL are 0.15 nm ± 27 pm and 0.41 ± 0.23 nm/h respectively. Both the resolution and the stability of the HCGIL are two orders of magnitude better than that of the HP5529A in a general uncontrolled laboratory environment.

Acknowledgments

This study was supported in part by the National Science Council of the Republic of China (Contract No. NSC 98-2218-E-032-009-, 99-2628-E-032-001-, and 100-2628-E-032- 001-).

#186589 - $15.00 USD Received 7 Mar 2013; revised 15 May 2013; accepted 17 May 2013; published 24 May 2013